Laser Physics, Vol. 12, No. 1, 2002, pp. 145–151.

The Escape Velocity in a Magneto-Optical Trap and Its Importance to Trap Loss Investigation

K. M. F. Magalhães, S. R. Muniz, G. D. Telles, Ph. W. Courteille, V. S. Bagnato, and L. G. Marcassa

Instituto de Física de São Carlos, Universidade de São Paulo, Caixa Postal 369, São Carlos-SP, 13560-970 Brazil

e-mail: srmuniz@if.sc.usp.br

Received May 18, 2001

Abstract—Using the dark spot slowing technique we have measured the capture velocity of a sodium magneto-optical trap as a function of trap laser intensity. The comparison with calculations based on a simple model allows us to obtain the escape velocity. Using this intensity dependent escape velocity and the Gallagher–Pritchard model [*Phys. Rev. Lett.*, **63**, 957 (1989)] we propose an alternative mechanism to explain the sudden raise up of trap loss rates at low intensity without relying on Hyperfine Changing Collisions.

1. INTRODUCTION

The ultracold collisions occupy an strategic position in the intersection of several important themes in the current research of atomic, molecular and optical physics. This position explains the wide interest and enormous growth of this field in the last decade. The good understanding of the atomic interactions was crucial in the evolution of many emerging and outstanding fields [1] such as Bose–Einstein condensation (BEC) in dilute alkali atoms, atomic interferometry, etc. Among the diverse types of experiments involving cold collision, trap loss measurements continue to produce important insights into the various inelastic process occurring in a sample of cold trapped atoms. In order to obtain a theoretical prediction for trap loss rates one has to make use of the escape velocity. Which is normally defined as the minimum velocity an atom has to acquire to escape from the radiative forces of the trap. The value of the escape velocity as a function of the laser intensity is normally obtained through a numerical simulation of a single atom embedded in a trap environment [1–4]. Although we believe that such simulation has produced satisfactory values for escape velocity, it has several limitations due to effects such as fluctuations, polarization imperfections, multi-level aspects of the atoms, etc. that are hard to be included in the calculations. To our knowledge, the only attempt to measure indirectly the escape velocity was done by Hoffmann and coworkers [5] using repulsive states excitation. The direct measurement of escape velocity is technically difficult and so far nobody yet has devised a scheme to perform such experiments. On the other hand, recently, we have develop a method to measure the capture velocity in a magneto optical trap [6, 7]. The capture velocity is usually defined as the maximum velocity an atom can come across the trap volume and still be captured into the trap. The capture velocity is closely related to the escape velocity and can be considered as its upper limit. So once the capture velocity (v_c) is measured, the escape velocity (v_{esc}) can be inferred.

We present in this paper the methodology used to measure the capture velocity and its extrapolation to the escape velocity in a sodium MOT. For this experiment, a new atomic beam deceleration method, called "dark-spot" Zeeman tuned slowing [8], was developed and will be also explained here. Finally we explore the importance of the escape velocity in the interpretation of trap loss at low light intensity [9], resulting in an alternative interpretation to the increase of trap loss rate that do not have to rely on Hyperfine Changing Collision as the main loss mechanism in this regime, and is still able to reproduce qualitatively the experimental results.

2. THE "DARK-SPOT" ATOMIC BEAM SLOWING FOR ON-AXIS LOADING OF OPTICAL TRAPS

To be able to measure the capability of the trap to capture atoms with different velocities, it is first necessary to develop the ability to control the velocity of the atomic flux used to load the trap. Several strategies have been employed to load MOTs from atomic beams that have been slowed using either the Zeeman tuning or frequency chirping technique Normally, the MOT is spatially offset from the axis of the slow atomic beam to avoid the strong unidirectional radiation pressure of the slowing laser, which greatly diminishes the MOT performance. This, however, does not result in efficient coupling of the flux of slow atoms into the MOT since, off axis, the MOT does not subtend very much of the solid angle of the slow atomic beam. Having the MOT on axis with the slowed atomic beam would greatly enhance the loading of atoms into the MOT. One strategy for on-axis loading employed an inverted Zeeman slowing field [10]. In this case, the slowing laser was sufficiently detuned from zero-field resonance to pre-

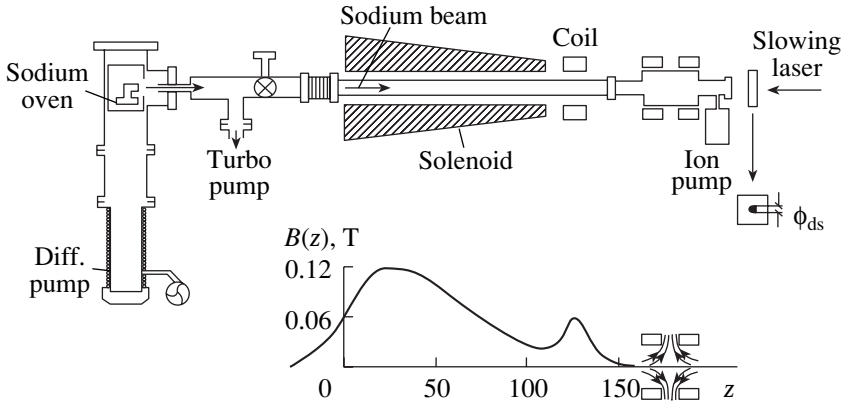

Fig. 1. (Top) Experimental setup. The beam, from an effusive sodium oven, is decelerated by the Zeeman tuning technique. The extraction coil modifies the slower field so that final deceleration of the atoms occurs closer to the MOT region. The MOT coils produce about a 0.1-T/m field gradient with currents such that they continue the field due to the slowing magnets. (Bottom) Magnetic-field profile. We have indicated the MOT coils field lines to show the continuation of the trapping field with the slowing field.

vent any influence on the MOT. This strategy, however, creates large magnetic fields near the exit end of the slower requiring that the MOT be placed further away, again reducing the solid angle of the slow beam subtended by the MOT. A variation of this strategy, involving a conventional Zeeman-tuned slower followed by a final section of inverted Zeeman slowing, also allows on-axis loading of a MOT [11], with smaller final magnetic fields. This scheme, however, requires the atoms to pass through a zero-magnetic-field region, before the final stage of slowing in the inverted Zeeman field, where optical pumping to other hyperfine levels can interrupt the slowing process, necessitating the use of additional laser frequencies to repump the atoms. Here we implement an alternative to conventional beam slowing and off-axis MOT loading. A dark spot placed in the center of the slowing beam makes a shadow on the position of the trap, allowing a large flux of slow atoms to be captured into the MOT without disturbing it. We have characterized this process using different dark-spot sizes and different slower laser frequencies and intensities. In order to determine the number and the density of trapped atoms, we measure the fluorescence from the atoms with a calibrated photomultiplier tube and we imaged the sample with a CCD camera. Under usual conditions, we load up to 1×10^9 atoms in the MOT.

A schematic of our experimental set up is presented in Fig. 1. Briefly, a sodium atomic beam from an effusive oven is directed into a tapered solenoid, which produces the Zeeman splitting necessary to compensate the Doppler shift, keeping the atoms in resonance with the slowing laser during all the deceleration process. The slowing laser beam comes from a Coherent 699-21 dye laser, passing through a lens system such that the beam is about 2 cm in diameter ($1/e^2$) at the entrance of the vacuum system, and it is focused at the nozzle of the oven (located about 250 cm down stream). The slowing solenoid field lines has the same direction as the field lines of the MOT quadrupole coils, so that the slow atomic beam does not pass through a zero-field region before the MOT. The trapping laser, from a second dye laser, is locked to a saturated absorption signal of a Na reference cell, shifted $\simeq -20$ MHz from the $3S_{1/2}$ ($F = 2$) $\longrightarrow$ $3P_{3/2}$ ($F' = 3$) transition by an acousto-optic modulator. An electro-optic modulator, at ~1712 MHz, is used to produce light at the $3S_{1/2}$ ($F = 1$) $\longrightarrow$ $3P_{3/2}$ ($F' = 2$) transition in order to repump atoms from the ground-state $F = 1$ hyperfine level.

To be able to efficiently load atoms into the MOT, the average velocity of the slow beam has to be less than the capture velocity of the MOT. In addition, it is desirable to stop the beam as near as possible to the MOT center, so that spatially the MOT can capture the atoms before they diffuse away. In our experimental setup, an extra coil is placed between the tapered solenoid and the trap. This coil allows us to extract a relatively slow beam from the tapered solenoid, with the final slowing of the atoms occurring at the end of the extra coil, near the trap. Without this extraction coil, atoms would, by off-resonant scattering of photons from the slowing laser in the decreasing fringing field of the tapered solenoid, continue to slow down, stop, and be turned around before they could reach the capture region of the MOT. The overall profile of the longitudinal magnetic field is shown in Fig. 1 (bottom), and details of how the extraction coil works can be found in [12].

Immediately before the vacuum chamber entrance window, the slowing laser passes through a glass slab that is mounted on an x–y translation stage. The glass slab is optically flat, antireflection coated on both sides, and has a dark (opaque) spot approximately in the middle of it. The diameter of the dark spot ϕ_{ds} can be varied from zero to about 10 mm (still smaller than the slower laser beam at this position, which is about 2 cm in diameter). The dark spot creates a shadow in the slowing laser beam. The position of the spot, relative to the

center of the laser beam, can be moved using the translation stage. This procedure is important to maximize the trap loading.

We clearly observe that the number of trapped atoms is strongly dependent with the dark spot size. This is basically due to two effects: changes in the loading rate or delivery of slow atoms to the MOT, and decreased performance of the MOT due to a force imbalance. The first effect has been studied extensively for Zeeman-tuned slowing [13–15]. The second effect is a consequence of on-axis loading of the MOT. The unidirectional light pressure exerted by the slowing laser passing through the MOT strongly unbalances the trapping forces, and causes the equilibrium position of the trapped atoms to move toward the oven. The displacement of the center of the trap from the zero-field position, produced by the quadrupole coils, is typically accompanied by poor MOT performance, resulting in a substantial reduction in the number of trapped atoms.

By monitoring the number of trapped atoms as a function of the spot size, we can obtain the optimum size to be used. Figure 2 shows the number of trapped atoms as the dark-spot diameter ϕ_{ds} is varied. Initially, as the spot diameter increases, the number of trapped atoms also increases. In this case, as we increase the size of the shadow, the deleterious influence of the slowing laser on the MOT decreases and more slow atoms can be accumulated. The maximum number is obtained at about ϕ_{ds} = 4 mm, after which the shadow along the whole slowing path starts to compromise significantly the slowing process, and the amount of captured atoms decreases again. For a larger ϕ_{ds}, atoms are slowed only near the edges of the capture volume, which does not correspond to very efficient loading. Under optimum conditions we are able to load ~30 times more atoms than without dark spot, and this corresponds to over 300 times more the number of atoms obtained when the same trap configuration (laser beam diameter, intensity, magnetic field, etc.) is used in a vapor cell MOT.

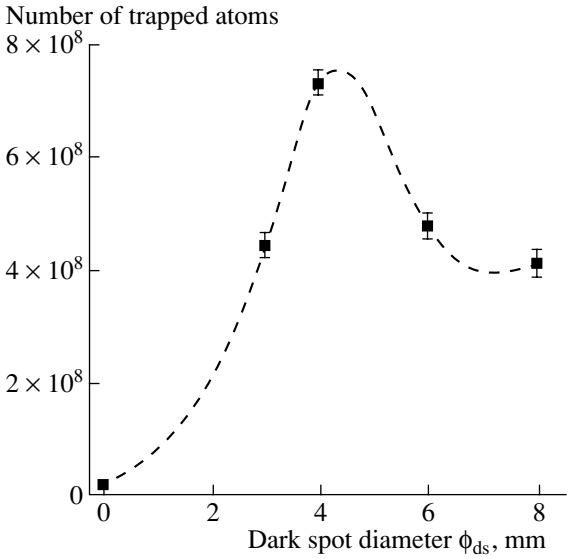

Fig. 2. Variation of the number of trapped atoms in the MOT as a function of the dark-spot diameter (ϕ_{ds}) placed in the slowing-laser beam. The points are averages of several measurements. The slowing beam diameter at the position of the dark spot is about 2 cm. The dashed line is a spline to connect the points and serves only to guide the eye.

3. OUTPUT VELOCITY DISTRIBUTION OF THE SLOWING PROCESS

In order to investigate the capturing properties of the MOT using a slowed atomic beam, it is necessary to know the characteristics of the velocity distribution. To characterize the output of the slowing process, we have used a probe laser beam generated by an extra dye laser. It crosses the atomic beam at a small angle about 30 cm away from the slowing solenoid exit and its low intensity does not affect the slowing process. The probe beam is mechanically chopped and the fluorescence is imaged onto a photomultiplier tube and the signal processed by a lock-in amplifier. The analyses of the fluorescence as a function of the probe laser frequency allow us to monitor the velocity distribution after the deceleration, as well as the emerging population in each of the two ground state sub-levels (F = 1 and F = 2). As previously, the observed output velocity distribution shows a velocity bunching towards low velocities. For slowing laser detunings (from –100 to 0 MHz) the emerging slow atomic flux is mainly composed of atoms in the F = 1 ground state (even thought the deceleration cycles atoms using the F = 2 ground state). The reason for this optical pumping effect is that as the slow atoms approach the solenoid exit, the magnetic field became small and the field lines diverge from the center, promoting an efficient optical pumping to the F = 1 state. This effect abruptly terminates the deceleration process and these very slow atoms migrate out to the solenoid exit region. We have measured with the probe laser the peak and the width of the outcoming velocity distribution. The final velocity peak basically obeys the relation $v_{out} = -\Delta/k$. This is because in the Zeeman tuned technique the changing Doppler effect is continuously compensated by changing magnetic field through a Zeeman adjustment of the transition frequency, the atomic longitudinal velocity at each point, for the atoms already resonant, is given by:

$$kv(z) = -\Delta + \gamma B(z), \qquad (1)$$

where Δ is the detuning of slowing laser, $k = 1/\lambda$ is the reduced wave vector of light.

With respect to the final width of the velocity distribution, we observed that it is close to a Gaussian and it presents a minimum width around Δ = –50 MHz, which corresponds to a velocity width of about 30 m/s, growing in value as we deviate from this detuning. Since we will be working in the interval from Δ = 0 to –100 MHz the velocity width is, therefore, between 30 to 40 m/s.

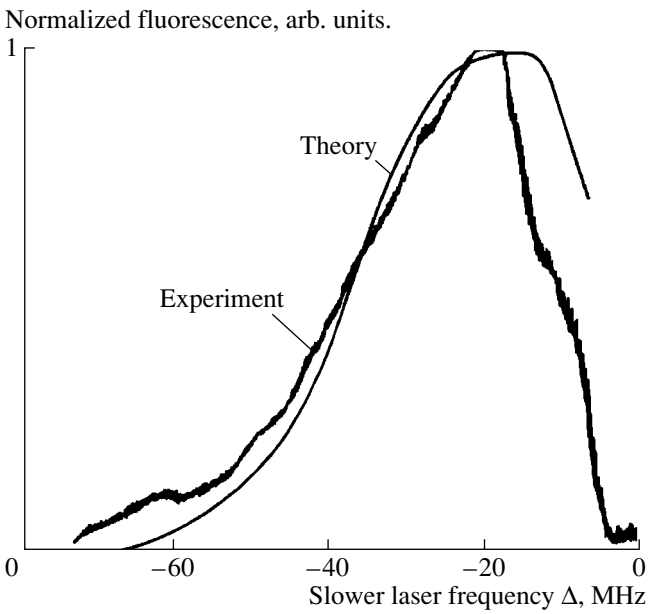

Fig. 3. Comparison between the measured number of captured atoms and the calculated signal. Both curves have been normalized for comparison.

These values will be used further in the determination of v_c.

4. MEASURING THE CAPTURE VELOCITY AND OBTAINING THE ESCAPE VELOCITY

The capture velocity (v_c) is dependent on the trapping parameters: intensity, detuning, laser beam size (capture volume) and magnetic field gradient. We observe the fluorescence from the trap as the frequency of the slowing laser is scanned. As the slowing laser frequency is scanned we are providing different velocity classes to be captured by the MOT, as previously characterized. Scanning the slower frequency from red to blue detunings, we observe a signal that slowly grows and it is followed by drop. This is presented as the experimental curve in Fig. 3. As the slowing laser frequency moves towards the resonance frequency, slower atoms are coming out. When a considerable amount of slow atoms are within the capture range of the MOT, the fluorescence starts to increase, denoting more capture. The amount of captured atoms keeps increasing as function of the slowing detuning, reaches a maximum and decreases afterwards. While the increasing is associated with more slow atoms within the capture range, the decrease arises from two effects. First, the outcoming velocity is getting close to zero and part of the distribution is reversing its velocity, been pushed back before getting into the MOT capture volume. Second, as the atoms come out slower, they have more time to diffuse out of the capture volume and a larger number of atoms are lost. Both processes diminish the loading rate of the MOT, causing the drop in the atom number. We have observed that the position and overall shape of the spectrum in Fig. 3 remains the same when the slower intensity is varied, only its amplitude varies in this case. This shows that the frequency of the slowing laser is the main control parameter for the loading process here.

The experimental data presented in Fig. 3 allows us to determine the value of the capture velocity. To extract v_c from the data, we consider the flux of slow atoms provided by the atomic beam as having a Gaussian velocity distribution, $g(v) = Ae^{-(v-v_f)^2/\sigma^2}$ (A is a normalizing constant), with the final velocity $v_f \sim -\Delta/k$ and $\sigma = \frac{\Delta v}{2}$ where Δv is the width of the distribution (30 m/s). Considering that we can capture all the atoms with velocity between 0 and v_c, the number of captured atoms (N_c) is given by

$$N_c = A\int_0^{v_c} e^{-\left(v+\frac{\Delta}{k}\right)^2/\sigma^2} dv. \qquad (2)$$

For different capture velocities, Eq. (2) predicts a different peak position and width for the number of trapped atoms. As the capture velocity decreases, the peak of the captured number is shifted towards smaller detunings. To determine v_c, we have fitted the rising part of the experimental spectrum of Fig. 3 with the expression provided by Eq. (2). The theoretical fitting is also shown in Fig. 3. The process is repeated for several trap laser intensities and v_c as a function of total trap intensity is obtained.

In Fig. 4 we show the experimental results for the capture velocity as a function of trapping light intensity (the dotted line is only for eye guidance), from 0 to 400 mW/cm^2. The intensity dependence has the expected behavior: it goes to zero with a rate that increases as the intensity decreases. In Fig. 5 we show the comparison between experimental and theoretical result for the low intensity regime. The theory consists in a three dimensional model where the radiative forces involving in the trap, due to all the laser beams, are considered within the Doppler Theory [16]. The maximum velocity that can be captured will always exceed the minimum velocity that can escape (escape velocity) because in the capture process the radiative force acts over the diameter of the capture volume, while in the escape the force acts over the radius only. For a given intensity of the trapping laser, the escape velocity (v_{esc}) is determined by considering initially an atom at the center of the trap and verifying the minimum velocity necessary to the atom escape. The calculation is done in several directions and the results averaged, producing the escape velocity for each laser intensity. For the capture velocity (v_c) the simulation consists of sending an atom across the trap configuration with some given velocity and verifying the maximum velocity in which

the atom is still captured. Averaging these values for several initial direction we obtain the calculated capture velocity. In this simulation we have varied the laser intensity and kept the detuning, beam size and magnetic field to the experimental values already provided. From the model we obtain a good approximation for the escape velocity $v_{esc} \sim 0.7 v_c$. Since the model is able to predict quite well the overall behavior of the capture velocity, we can use this correction factor in the data of Fig. 4 to obtain a possible dependence of the escape velocity as a function of trap light intensity.

The final result is that as the intensity increases from zero up, v_{esc} also increases, reaching a maximum and decreasing back slowly. The first part is compatible with the potential becoming deeper as the intensity increases. After the maximum, the observed decrease in v_{esc} is probably due to power broadening of the atomic transition. Such that under high intensity, the atom can not distinguish the radiative forces of both counter propagating laser beams; causing a decrease of the viscous force and consequently on v_{esc}.

For a fixed high light intensity (320 mW/cm^2) in the MOT, we have repeated the experiment varying the magnetic field gradient of the MOT coils The obtained result for the escape velocity as a function of magnetic field gradient is shown in Fig. 6. This result indicates an important tendency: as the magnetic field gradient decreases, the escape velocity seems to become a constant, independent of the field gradient. This suggests that for a conventional trapping conditions (~10 G/cm) both, the capture and escape velocities are more dependent of the viscous component of the radiation force than the restoring trapping force.

5. CONSEQUENCES OF THE ESCAPE VELOCITY KNOWLEDGE ON THE TRAP LOSS INTERPRETATION

Collision mechanisms involving kinetic energy release were among the first concerns in the study of optical traps [17]. Measurements of the intensity dependence of trap loss rate [18–22] suggested that there are three collisional processes which produces losses in a MOT: Radiative Escape (RE), Fine Structure Change Collision (FSC) and Hyperfine Change Collision (HCC). At high trapping intensity, only RE and FSC can contribute to trap loss because the kinetic energy gained by the atomic pair in both processes is larger that the trap depth. These processes present a very characteristic intensity dependence, their rates increases as the light intensity increases, because they involve a ground-excited atomic pair. If the number of excited atoms increases with the light intensity, the number of colliding (ground-excited) pairs will also get larger and therefore their loss rates. However, the trap depth also varies as the trap laser intensity decreases, and it is possible to reach a situation when the trap potential becomes shallower and eventually the energy gained during HCC is enough to overcome the trap depth. This effect will increase the total loss rate relatively fast below certain intensity, reaching a constant value. This explanation for the intensity dependence of the trap loss rate was first proposed by Sesko *et al.* [18], and it has been accepted and used in other alkali systems [19–22]. The contribution of each collisional process to the total trap loss rate depends on one trapping parameter, the trap depth, which is directly connected to the escape velocity. Therefore, the knowledge of the escape velocity is fundamental to understand the intensity dependence of trap loss rate.

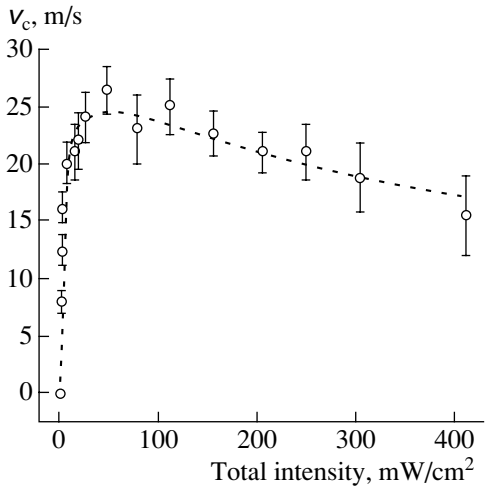

Fig. 4. Measured capture velocity as a function of trapping laser intensity for a detuning $\Delta \sim -10$ MHz, half waist of the Gaussian beam of 4.5 mm and $\frac{dB}{dz}$ = 15 G/cm. The dotted line used to connect the experimental points is just for eye guidance.

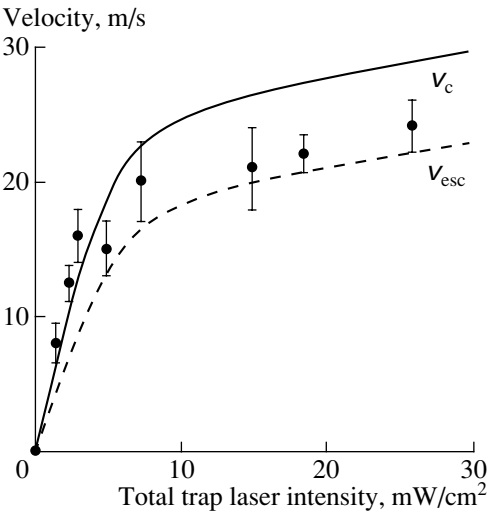

Fig. 5. Calculated escape (v_{esc}) and capture (v_c) velocities together with the experimental points in the region of low intensities.

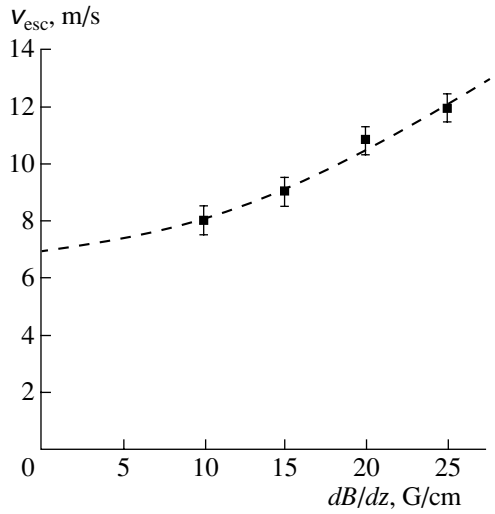

Fig. 6. Escape velocity as a function of the MOT magnetic field gradient. The dashed line is just an eye guide.

However, in two recent experiments trap loss rate was measured in a low intensity regime and a strange behavior was observed. Bradley and co-workers [23] measured trap losses in a Cr MOT. The rate coefficient, β, at the studied intensity range presented similar behavior when compared to the results obtained with other alkali atoms. Nevertheless, the absence of hyperfine structure in Cr atoms can not support HCC as the main mechanism causing losses on that system. Another significant result was recently provided by Nesnidal *et al.* [24], where the collisional loss rates due to spin-exchange at very low intensities were experimentally investigated. In brief, they observed that β reaches a maximum as intensity is decreased, starting to drop towards zero for lower intensities. Considering that spin-exchange is actually the main loss mechanism at low trap intensity, they concluded that the low light field qualitatively and quantitatively changes the behavior of spin-exchange collisions. Both results [23, 24] indicate the lack of understanding about trap loss rates at low light intensity.

In recent paper [9] we proposed an alternative interpretation for the intensity dependence of trap loss rate β without relying on hyperfine change collision as the dominant mechanism at low intensities. Our model is based on the Gallagher–Pritchard theory [25], normally referred to as the GP model, associated with a escape velocity dependent on the light intensity, as presented here. The GP model can be divided in two steps. In the first step, it is considered the excitation of the colliding pair to an attractive $1/R^3$ potential. In the second step, it is considered the atomic motion in this potential and the probability that the atomic pair will survive to spontaneous decay, reaching short internuclear separation, where RE may take place and lead to losses. The escape velocity determines at which internuclear separation RE can provide energy enough for the atoms to escape from the MOT. Using this simple theory we are able to reproduce qualitatively the intensity behavior of β, including the recent measurements by Nesnidal *et al.* [24]. We were also able to predict the intensity where the minimum in β is experimentally observed. The agreement between the prediction and the present model is quite remarkable. Nevertheless, we believe that a better agreement would be obtained if the escape velocity could be measured directly rather than calculated or inferred from the capture velocity measurements.

6. CONCLUSIONS

In conclusion, we have experimentally measured the capture velocity as a function of trap laser intensity in a sodium MOT. We have used a dark spot slowing technique, which allows us to vary the velocity of the atomic flux provided to be trapped, without disturbing the trap performance. Our results are in good agreement to the prediction obtained using a simple model. Using this model and the experimental data for the capture velocity, we were able to infer the escape velocity intensity dependence. The GP model associated with a escape velocity dependent on the light intensity is able to explain the high trap loss obtained at low laser intensity without relying on the occurrence of hyperfine change collisions. Simply, the intensity variation of escape velocity introduces variation on the probability of radiative escape, taking to a sudden increase in β as the intensity is lowered. It is important to say that the actual contribution of HCC at low intensity and the dependence of the escape velocity still remain to be measured directly.

ACKNOWLEDGMENTS

This work has received support from Fapesp (Programa de Centros CEPID—Centro de Pesquisa em Óptica e Fotônica CePOF) and Programa Pronex-CNPq.

REFERENCES

1. Weiner, J., Bagnato, V.S., Zilio, S.C., and Julienne, P., 1999, *Rev. Mod. Phys.*, **71**, 1.
2. Marcassa, L.G., Bagnato, V.S., Wang, Y., *et al.*, 1993, *Phys. Rev. A*, **47**, R4563.
3. Wallace, C., Dinneen, T., Tan, K., *et al.*, 1992, *Phys. Rev. Lett.*, **69**, 897.
4. Ritchie, N.W.M., Abraham, E.R.I., Xiao, Y.Y., *et al.*, 1995, *Phys. Rev. A*, **51**, R890.
5. Hoffmann, D., Bali, S., and Walker, T., 1996, *Phys. Rev. A*, **54**, R1030.
6. Bagnato, V.S., Marcassa, L.G., Miranda, S.G., *et al.*, 2000, *Phys. Rev. A*, **62**, 013404-1.
7. Muniz, S.R., Magalhães, K.M.F., Courteille, Ph.W., *et al.*, 2001, LANL e-print archives: physics/0104051.

8. Miranda, S.G., Muniz, S.R., Telles, G.D., *et al.*, 1999, *Phys. Rev. A*, **59**, 882.
9. Telles, G.D., Bagnato, V.S., and Marcassa, L.G., 2001, *Phys. Rev. Lett.*, **86**, 4496.
10. Barrett, T., Dapore-Schwartz, S., Ray, M., and Lafyatis, G., 1991, *Phys. Rev. Lett.*, **67**, 3483.
11. Witte, A., Kisters, T., Riehle, F., and Helmcke, J., 1992, *J. Opt. Soc. Am. B*, **9**, 1030.
12. Firmino, M.E., Faria Leite, C.A., Zilio, S.C., and Bagnato, V.S., 1990, *Phys. Rev. A*, **41**, 4070.
13. Napolitano, R.J., Zilio, S.C., and Bagnato, V.S., 1990, *Opt. Commun.*, **80**, 110.
14. Bagnato, V.S., Salomon, C., Marega, E., and Zilio, S.C., 1991, *J. Opt. Soc. Am. B*, **8**, 497.
15. Napolitano, R.J. and Bagnato, V.S., 1993, *J. Mod. Opt.*, **40**, 329.
16. Cook, R.J., 1979, *Phys. Rev. A*, **20**, 224.
17. Prentiss, M., Cable, A., Bjorkholm, J.E., *et al.*, 1988, *Opt. Lett.*, **13**, 452.
18. Sesko, D., Walker, T., Monroe, C., *et al.*, 1989, *Phys. Rev. Lett.*, **63**, 961.
19. Marcassa, L.G., Bagnato, V.S., Wang, Y., *et al.*, 1993, *Phys. Rev. A*, **47**, R4563.
20. Shang, S.Q., Lu, Z.T., and Fredman, S.J., 1994, *Phys. Rev. A*, **50**, R4449.
21. Santos, M.S., Antunes, A., Nussenzveig, P., *et al.*, 1998, *Laser Phys.*, **8**, 880.
22. Wallace, C., Dinneen, T., Tau, K., *et al.*, 1992, *Phys. Rev. Lett.*, **69**, 897.
23. Bradley, C.C., McDeland, J.J., Anderson, W.R., and Cellota, R.J., 2000, *Phys. Rev. A*, **61**, 053407.
24. Nesnidal, R.C. and Walker, T.G., 2000, *Phys. Rev. A*, **62**, 030701(R).
25. Gallagher, A. and Pritchard, D.E., 1989, *Phys. Rev. Lett.*, **63**, 957.